Detection of secreted peptides by using hypothesis-driven multistage mass spectrometry

Markus Kalkum*, Gholson J. Lyon†, and Brian T. Chait*‡

*Laboratory of Mass Spectrometry and Gaseous Ion Chemistry and †Selma and Lawrence Ruben Laboratory of Synthetic Protein Chemistry, The Rockefeller University, 1230 York Avenue, New York, NY 10021

Edited by Fred W. McLafferty, Cornell University, Ithaca, NY, and approved January 2, 2003 (received for review October 30, 2002)

A method is presented for the rapid detection and characterization of trace amounts of peptides secreted from microorganisms, including pheromones, virulence factors, and quorum-sensing peptides. The procedure, based on targeted multistage MS, uses a novel matrix-assisted laser desorption/ionization-ion trap mass spectrometer to overcome limitations of current MS methods (limited dynamic range, signal suppression effects, and chemical noise) that impair observation of low abundance peptides from complex biological matrixes. Here, secreted peptides that are hypothesized to be present in the supernatant, but that may not be sufficiently abundant to be observed in single-stage mass spectra, are subjected to multistage MS. Highly specific fragmentation signatures enable unambiguous identification of the peptides of interest and differentiation of the signals from the background. As examples, we demonstrate the rapid (<1 min) determination of the mating type of cells in colonies of *Saccharomyces cerevisiae* and the elucidation of autoinducing peptides (AIPs) from supernatants of pathogenic Staphylococci. We confirm the primary structures of the *agrD* encoded cyclic AIPs of *Staphylococcus aureus* for groups I, II, and IV and provide direct evidence that the native group-III AIP is a heptapeptide (INCDFLL). We also show that the homologous peptide from *Staphylococcus intermedius* is a nonapeptide (RIPTSTGFF) with a lactone ring formed through condensation of the serine side chain with the C terminus of the peptide. This is the first demonstration of cyclization in a staphylococcal AIP that occurs via lactone formation. These examples demonstrate the analytical power of the present procedure for characterizing secreted peptides and its potential utility for identifying microorganisms.

Assays that provide information on specific peptides that are secreted by living cells (e.g., toxins, pheromones, virulence factors, and quorum-sensing peptides) can be valuable as diagnostic aids. For example, the presence and identity of a specific microorganism may be inferred by detection of characteristic secreted peptides, which may also be used to distinguish between subtypes of a given strain. Several authors have described the use of MS to identify microorganisms based on fingerprint masses of protein constituents as well as secreted peptides and proteins (1). Recently, electrospray ionization-Fourier transform tandem MS (MS/MS) of intact proteins has been applied for the characterization of biomarkers from *Bacillus cereus* T spores (2), and a combined approach of single-stage MS and MS/MS was used to identify proteins secreted from adipocytes (3). Because these methods rely on the initial detection by single-stage MS of intact peptide ions from a highly complex milieu, it may be difficult to detect trace amounts of the secreted peptides. In addition to limitations imposed by dynamic range and signal suppression effects, low-level signals of interest tend to disappear into the "chemical noise" (4–6). An approach that has been widely applied with great success to the detection of trace compounds in complex mixtures involves MS/MS (7) by using targeted compound analysis (reviewed in ref. 8). Here, we present a method building on these previous approaches for the rapid, unambiguous detection of trace amounts of peptides secreted from microorganisms, by using multistage MS (MS^2 and MS^3) analysis of crude supernatant mixtures with a novel matrix-assisted laser desorption/ionization (MALDI)-quadrupole ion trap mass spectrometer (9). In this procedure, secreted peptide ions that are hypothesized to be present in the supernatant, but that are not sufficiently abundant to be observed in the regular single-stage mass spectra, are subjected to multistage MS. Highly specific fragmentation signatures enable unambiguous identification of the peptides of interest and differentiation of the signals from the background. As examples, we demonstrate the rapid determination of the mating type of colonies of *Saccharomyces cerevisiae* and the detection and structural characterization of autoinducing peptides (AIPs) of *Staphylococcus aureus* that play a crucial role in quorum sensing and bacterial interference.

Haploid yeast cells secrete one of two types of peptide pheromones, i.e., mating factors **a** or α (10–12). Their expression is controlled (but not encoded) by the alleles at the mating type loci *MAT***a** or *MAT*α. *MAT***a** cells secrete mating factor **a**, which binds to a receptor on the surface of *MAT*α cells, and *MAT*α cells secrete mating factor α, which binds to a receptor on the surface of *MAT***a** cells. Receptor binding of a mating factor triggers the mating response, i.e., activation of proteins required for cell fusion (13–15). Knowledge about the presence of a specific mating factor is an indicator of a haploid strain, information that is essential when designing mating experiments for genetic studies. Current mating type assays use methods that challenge the strain in question with tester-strains (16) or that analyze it by PCR (17). These assays require overnight incubation (18) and, so, are relatively slow (16, 19). Here, we demonstrate a rapid method for determining the mating type in yeast.

Virulent *S. aureus* is an invasive pathogen that can infect almost any human tissue. It has the potential to provoke several forms of human disease, including food poisoning (20), skin infections (21), endocarditis (22), and toxic shock syndrome (23). Secreted proteins like the Staphylococcal enterotoxins belong to a family of so-called superantigens that share the ability to trigger excessive and aberrant activation of T cells manifested in various symptoms from atopic dermatitis (24) to toxic shock syndromes (23). Cell density-dependent peptide quorum sensing (25–28) controls the secretion of these toxins, as well as a variety of other virulence factors and surface proteins. The *agr* locus of *S. aureus* (and the staphylococci in general) encodes the components *agrB*, *D*, *C*, *A*, and *rnaIII* for such a peptide quorum-sensing system (29). AgrB is presumed to process the propeptide precursor AgrD to form the mature autoinducing peptides (AIPs) (30), which are characterized by a thiolactone structure comprised of a pentapeptide ring formed through condensation of the sulfhydryl group of a cysteine with the α-carboxyl group of the C-terminal amino acid. These lariat-like structures are called autoinducing peptides because they stimulate gene expression of several exported proteins as well themselves when they bind to

This paper was submitted directly (Track II) to the PNAS office.

Abbreviations: MALDI, matrix-assisted laser desorption/ionization; MS/MS, tandem MS; MS^n, *n*-stage MS; Mf, mating factor; AIP, autoinducing peptide.

‡To whom correspondence should be addressed. E-mail: chait@rockefeller.edu.

the receptor-histidine kinase, AgrC (30, 31). The *agr* locus is hypervariable leading to variations in *agrD*, *B*, and *C* that classify *S. aureus* into four different *agr* groups (32) [and >20 other putative *agr* groups in other staphylococcal species (33)]. AIPs from one group usually cross-inhibit virulence specific gene expression in *S. aureus* strains from a different group, and supernatants of other staphylococcal strains usually inhibit activation in *S. aureus* (34). This form of bacterial interference (34, 35) is thought to be of clinical relevance in infection and colonization. Thus, a rapid and reliable method to detect and distinguish between different staphylococcal strains based on which AIPs they secrete is potentially of great diagnostic utility.

Materials and Methods

Strains, Media, and Culture Conditions. *W303 MAT***a**, *MATα*, and 2N genetic background: *ade2-1 ura3-1 his3-11,15 trp1-1 leu2-3,112 can1-100*; *YW046 MAT***a** and *MATα* with genetic background: *ura3Δ5 leu2-3,112 his3 pra1-1 prb1-1 prc1-1 cps1-3* both from M. P. Rout (The Rockefeller University, New York); *BY4741 MAT***a** with *his3Δ1 leu2Δ0 met15Δ0 ura3Δ0* (ResGen, Invitrogen); and crosses thereof with the first two strains. The yeast strains where grown on YPD plates (1% yeast extract, 2% peptone, 2% Bacto agar, and 2% D-glucose) at 30°C.

S. aureus strains used were: RN6734 (group-I AIP), RN6607 (group-II AIP), RN8465 (group-III AIP), and RN4850 (group-IV AIP) (36). The *S. intermedius* strain RN9423 was kindly provided by G. Lina (Faculté de Médecine Laennec, Lyon Cedex, France).

Preparation of AIP-Containing Supernatants. *S. aureus* strains were grown in CYGP broth (10 g/liter casamino acids/10 g/liter yeast extract/5 g/liter glucose/5.9 g/liter NaCl/60 mM β-glycerophosphate; ref. 37) with shaking at 37°C for 9 h starting with an inoculum of $\approx 1.5 \times 10^7$ cells per ml in 5 ml of broth. Cells were removed by centrifugation at 4°C, and the supernatant was filtered (0.22-μm filter, Gelman).

Synthetic Peptides. The synthetic AIPs used in this study have been described (38, 39). Mfα and Mf**a** were both purchased from Sigma.

MS. The MALDI-quadrupole ion trap was constructed from a Thermo Finnigan LCQ Deca XP (San Jose, CA) as described for the earlier LCQ version (9). Short ion injection times (typically 0.3–5.0 ms) were used for single-stage MS experiments to prevent overfilling effects. MS/MS and MS^3 experiments were performed at longer injection cycles (200–400 ms) by using empirically optimized instrument specific parameters (isolation width: 2.0 Da, normalized collision energy: 30% for yeast Mfs, and 35% for AIPs, activation Q: 0.240, activation time: 300 ms). Spectral acquisition times varied from 30 s to 1 min to achieve acceptable signal:noise ratios.

Sample Preparation for MS. A needle tip amount of a yeast colony (1–3 mg of the strains listed above) was transferred into 5 μl of half-saturated solution of 2,5-dihydroxy benzoic acid in 60% methanol/0.1% trifluoroacetic acid. After vortexing the sample, cells were spun down by using a tabletop centrifuge. Up to 2.5 μl of the supernatant was transferred onto the MALDI compact disk (CD)-sample plate (9) and dried. Note: When screening for Mfα-producing cells only, stronger ion intensities were obtained when the cells were suspended in 0.1% trifluoroacetic acid lacking the organic solvent. In this case, saturated 2,5-dihydroxy benzoic acid matrix solution was added after deposition of the sample on the CD.

Approximately 0.5 ml of Staphylococcal culture supernatant was lyophilized and resuspended in 100 μl of 1% trifluoroacetic acid to which was added 5 μl of a suspension of hydrophobic Poros 20 R2 beads (PerSeptive Biosystems, Framingham, MA) in 10-fold bed volume of 2% formic acid. Using a 1-ml disposable syringe and a self-made adapter piece (cut from a P200 pipette tip) a portion or the entire sample was squirted through a ZipTip microcolumn (Millipore) that also served as a frit for the Poros material. The column-bound material was washed with 20 μl of 0.1% trifluoroacetic acid before eluting it directly onto the MALDI CD-plate by using 2.5 μl of half-saturated 2,5-dihydroxy benzoic acid solution (see above). Synthetic peptides were simply spotted onto the MALDI CD-plate in 1-μl volumes of 1 nM solutions (or a dilution series) to which 1 μl of matrix solution were added subsequently.

Results

Hypothesis-Driven MS/MS Analysis of Yeast Mating Factors (Mfs). The left spectra in Fig. 1 show partial MALDI mass spectra of the extracts obtained by placing a small quantity of each of the three cell types in the MALDI matrix solution. The mass spectra encompass the region m/z 1,550–1,750, where we expect to observe the Mf peptides. In no case do we observe the Mf peptides in these single-stage mass spectra, so that it is not possible to judge whether they are present or not. Indeed, the spectra are highly congested, with just a few peptide ion peaks apparent over the background. These more intense peptide ions, although not identified, are not characteristic of the different mating types because they appear in all three spectra.

In the hypothesis-driven MS/MS experiment, the ion trap is set to eject all ions except those that correspond to the theoretical m/z values of the Mfs. In this way, specific ions that are hypothesized to be present are isolated and subjected to MS/MS analysis (Fig. 1). Fig. 2 shows MS/MS analysis of synthetic Mf**a** and Mfα, where as expected the fragmentation is highly characteristic of each peptide. Specifically, the most intense ions correspond to the described preferred cleavages of singly charged ions in the ion trap mass spectrometer, i.e., on the C-terminal side of Asp and N-terminal side of Pro residues (40, 41). These intense fragment-ion signals define MS/MS signatures, which unambiguously identify the mating factors and distinguish their ions from background ions at the same mass (Fig. 1). Thus, crude extracts from *MATα* cells produce a diagnostic MS/MS spectrum when parent ions are selected at m/z 1,683.9, the calculated m/z of Mfα (Fig. 1 *Top*, right spectrum), but no fragmentation characteristic of Mfs are observed when parent ions are selected at m/z 1,629.9 or 1,643.9, the calculated m/zs of Mf**a** (42) and its variant (43) Mf**a′** (Fig. 1 *Top*, center two spectra). In the same way, MS/MS with samples of *MAT***a** cells yield diagnostic spectra when parent ions are selected at m/z 1,629.9 and 1,643.9, corresponding respectively to the calculated masses of Mf**a** and Mf**a′** (ref. 44; Fig. 1 *Middle*, two center spectra). In contrast to our observations with haploid cells, no MS/MS fragmentation characteristic of the mating factors is obtained from diploid cells (*MAT***a**/α, Fig. 1 *Bottom*). Thus, by simply performing MS/MS analysis on the three hypothetically present Mfs, we can quickly determine which Mf is present in the colony of interest. Signal intensities for the Mf**a** and **a′** were observed at comparable levels, which may reflect equal expression levels of both encoding genes, *MFA1* and *MFA2* as reported (45). Similarly, there exists a variant counterpart of the *MFα1* gene termed *MFα2*, which encodes two copies of Mfα, one of which, Mfα′, varies by two amino acid residues (Q5N and K7R) (46) [note that *MFα1* encodes four identical copies of Mfα (47)]. In contrast to the similar expression levels of *MFA1* and *MFA2*, the *MFα2* gene does not contribute significantly to pheromone production (48). Accordingly, Mfα′ was not detected by the present method.

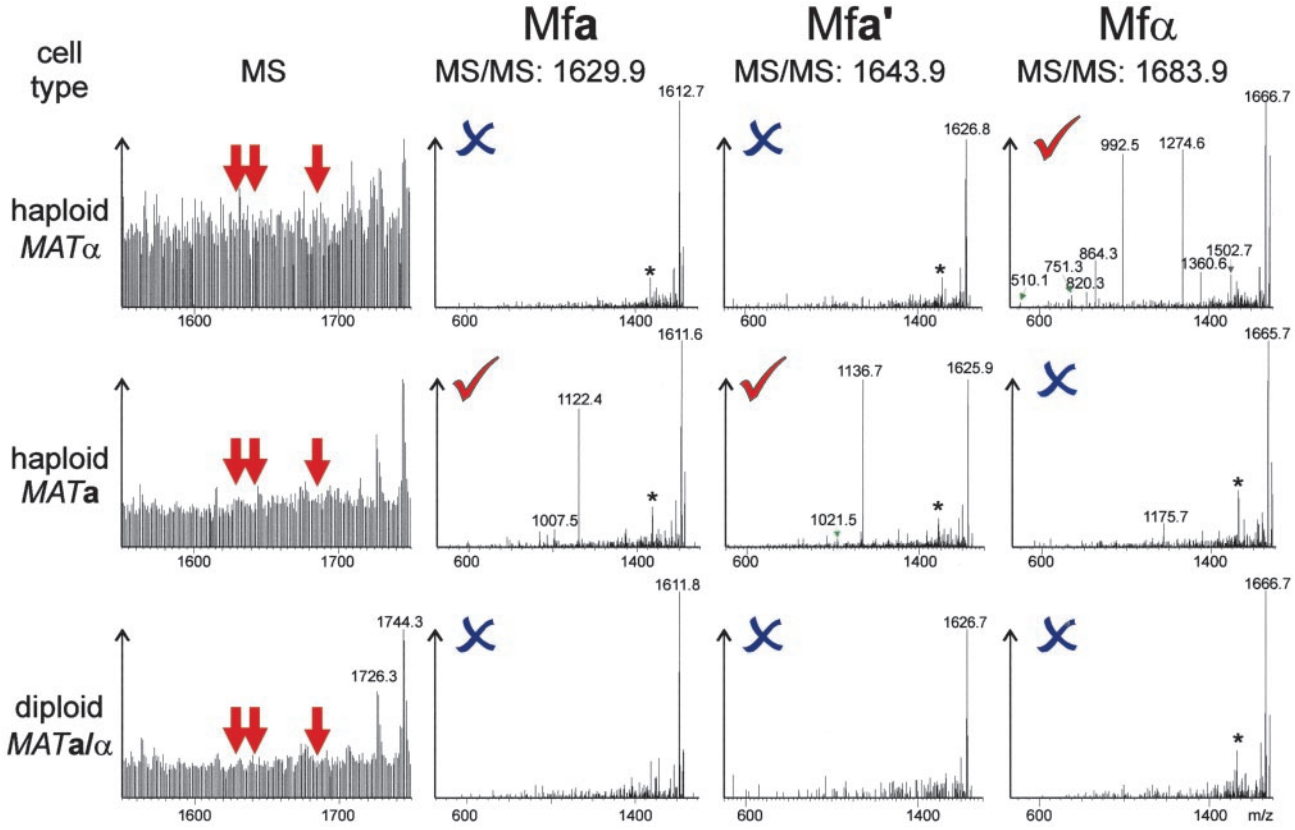

Fig. 1. Hypothesis-driven multistage MS screen for yeast-mating factors. MALDI-ion trap mass spectra obtained from samples of three different *S. cerevisiae* cell types: haploid *MAT*α, haploid *MAT***a**, and diploid *MAT***a**/α (no mating type). Mfs are not detected by single stage MS (left spectra). MS/MS experiments with ions selected at hypothetical *m*/*z* values (red arrows) reveal the presence of Mfs (red checkmarks). Only the most intense fragments are clearly seen above the noise (compare with Fig. 2 for other fragment ions). Mfα is only detected from *MAT*α cells (*Top*, right spectrum). Characteristic fragments for Mfa and variant Mfa' are only obtained with *MAT***a** cells (*Middle*, two center spectra), and no Mfs are detected with diploid cells (*Bottom*, blue crosses). Aside from broadly distributed noise, which is more intense close to the parent masses than in the lower mass range of a spectrum, some discrete peaks are designated as artifacts, i.e., the peaks at parent mass –18, and –136.6 (marked with ∗). Such signals are attributed to dissociated clusters of the MALDI matrix (4). The ordinate shows relative intensities.

Hypothesis-Driven n-Stage MS (MS^n) Analysis of Staphylococcal AIPs. Despite concentrating and desalting the culture supernatants of *Staphylococcus aureus*, it was not generally possible to decide on the presence or absence of AIPs based on the single stage MS spectra (Fig. 3 *Top Left* of I, II, III, and IV). Indeed, it proved necessary to perform both double-stage (MS/MS) and triple-stage (MS^3) experiments on synthetic AIPs to assess the most intense fragment-ions that should be expected when analyzing the naturally occurring AIPs from supernatants. For example, the fragmentation of synthetic group-I AIP ions yields an intense y_6 ion peak at *m*/*z* 711.5 and less intense y_5 and y_7 ion peaks at *m*/*z* 610.6 and 798.5, respectively (Fig. 3*I*). However, only the intense y_6 ion can be distinguished from the background noise in the MS/MS spectrum of natural group-I AIP supernatants. Indeed, because of residual background in the MS/MS spectrum, it proved necessary to perform a triple-stage MS experiment (MS^3) to test whether the peak at *m*/*z* 711.5 from the MS/MS experiment can be attributed with high confidence to AIP-I. The MS^3 experiment with the supernatant sample of group-I-AIP reveals essentially the same fragmentation pattern as that obtained with the corresponding synthetic peptide. In general, MS/MS fragmentation of groups I, III, and IV AIPs lead to fragment ions that retain the cyclic component of the intact peptides. Because two cleavages are necessary to obtain observable fragments from a ring, such fragment ions are first detected in the MS^3 experiments (Fig. 3).

A deviation from this scheme is observed for the group-II AIP. This peptide is predominantly desorbed as the singly natriated ion ($M+Na^+$) rather than the more commonly ob-

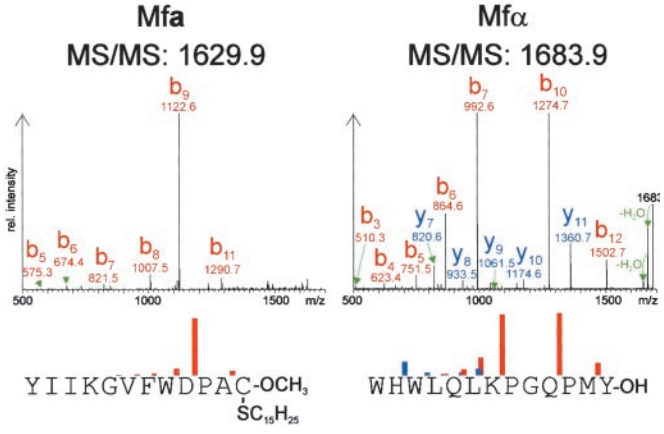

Fig. 2. MALDI-ion trap MS/MS spectra of synthetic yeast Mfa and Mfα. Assignment of sequence-specific MS/MS signatures is indicated by fragmentograms underneath [red bars indicate b ion (53) intensities and blue bars those of y ions (53)]. The synthetic variants, Mfα' and Mfa', were not available for this study (see Fig. 1 for natural Mfa').

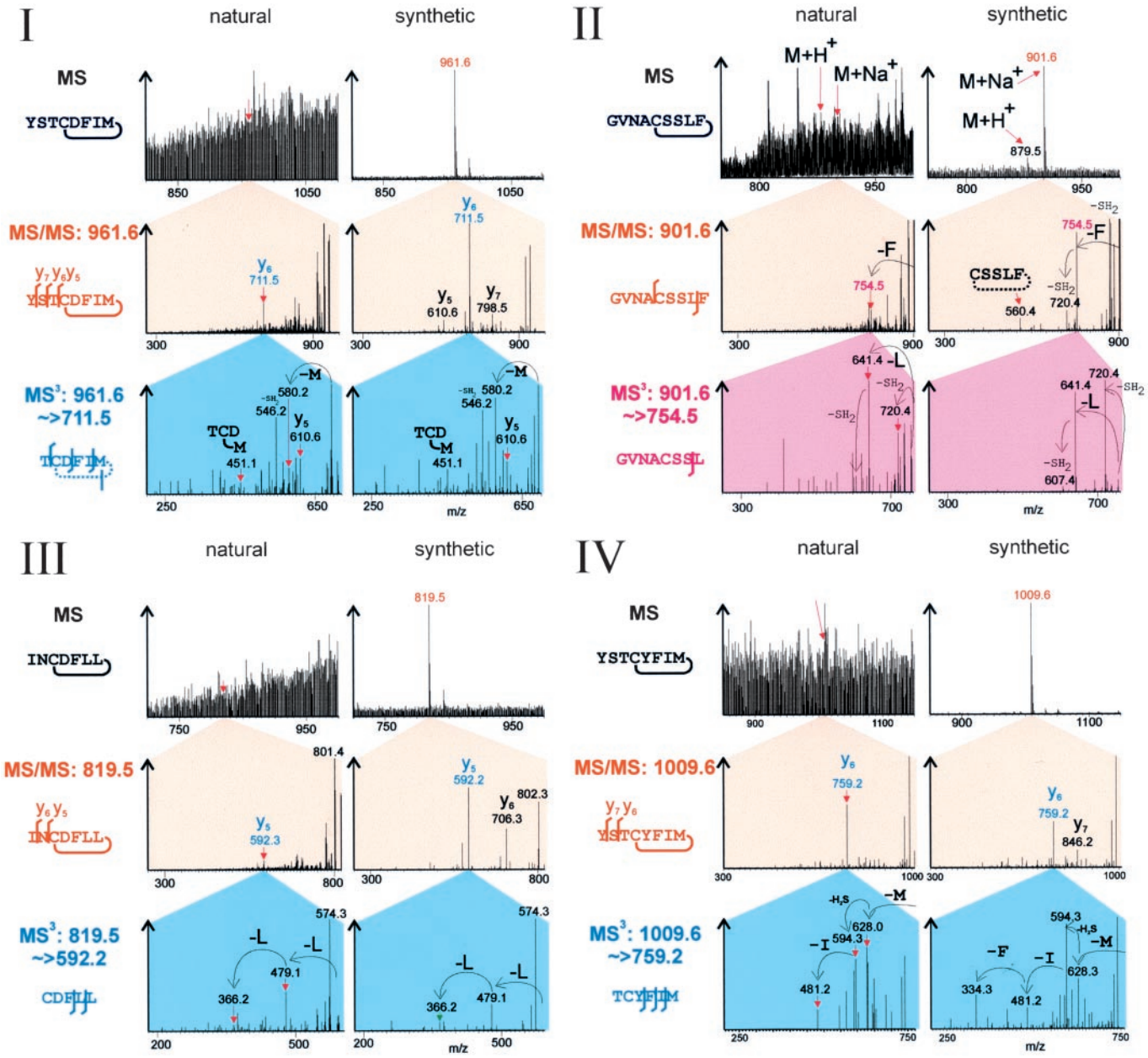

Fig. 3. Hypothesis-driven MS^n analysis of groups I–IV AIPs from *S. aureus* culture supernatants (natural) and comparison with MS^n spectra of synthetic AIPs. Only the most abundant fragmentation pathways of these lariat-like peptides are indicated. Note that MS/MS and MS^3 experiments for the group-II AIP were performed on the more abundant natriated ions ($M+Na^+$); all other spectra are those of protonated ions and their fragments. The tip of the beige background underlying the MS/MS spectra points to the parent ion. MS^3 spectra are marked in blue for parental y ions and in purple when derived from parental b ions.

served protonated form ($M+H^+$) (Fig. 3*II*, synthetic), even though the sample is prepared at low pH. Loss of phenylalanine in the MS/MS experiment indicates dissociation of the ring (Fig. 3*II*, ion peak at m/z 754.5), which is not observed when fragmenting the protonated synthetic peptide (data not shown). In this case, the polar serine residues in the ring appear to chelate the sodium cation, thus altering the fragmentation behavior. When we assumed that the hypothetical parent ion mass of the group-II AIP was natriated, we observed identical MS/MS and MS^3 fragment ions from the peptide presumed to be present in the culture supernatant as from the synthetic group-II AIP (Fig. 3*II*).

In all these examples, only the most intense MS/MS peaks can be used with confidence to verify the presence of AIP peptides in the supernatants; hence, only their m/zs were chosen for the MS^3 experiments. The MS^3 experiment was particularly necessary to unambiguously verify the presence of the natural group-III AIP because its diagnostic y_5 fragment is of relatively low intensity (Fig. 3*III*, natural). Moreover, in the original description of the AIP structures, the mature group-III AIP was assumed to be an octapeptide (34). However, when we tested for the presence of the peptide by using the published sequence and calculated mass, we did not find it. Consequently, we tested a number of other possibilities until we determined the correct structure. In this case, it proved necessary to test 28 different hypotheses derived from the precursor sequence, taking into account the different possible processing sites, the possible presence of a linear or a cyclized structure, and the possibility of

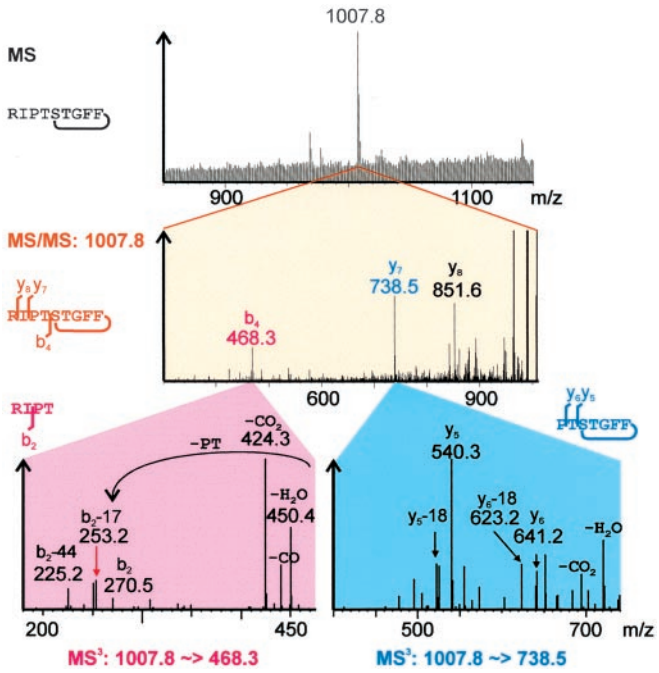

Fig. 4. MALDI-ion trap MS^n characterization of the *S. intermedius* AIP from culture supernatants. MS^3 spectra are marked in blue for parental y ions and in purple when derived from parental b ions. The AIP is a nonapeptide whose circular portion comprises a lactone.

preference for ionization by sodium cation (as it occurred for the group II autoinducing peptide) vs. protonation. This entire experiment was accomplished on a single MALDI sample in <15 min, with plenty of sample remaining should it have proved necessary to test more hypotheses. Our analysis indicated that the group-III AIP is a heptapeptide and not an octapeptide, as previously assumed (34). This observation corresponds well to recent findings, which demonstrate that only the synthetic heptapeptide, and not the octapeptide or nonapeptide, activates *agr* group-III cells (39).

The Cyclic AIP of *Staphylococcus intermedius* Is a Lactone. Fivefold concentrated, desalted culture supernatant of *S. intermedius* gave a clearly discernable signal at m/z 1,007.8 in the single-stage MS mode (Fig. 4). It would be possible to assign this signal to the AIP of *S. intermedius* if one assumes that the AIP is a nonapeptide and that cyclization is accomplished via a lactone bond rather than the previously discussed thiolactone (because the *S. intermedius* AIP contains a serine instead of a conserved cysteine residue at the corresponding position in all other AIPs examined). To test these hypotheses, multistage MS experiments were performed on the ions at m/z 1,007.8 and on fragments thereof (Fig. 4). Three fragments (y_8, y_7, and b_4) were obtained in the MS/MS experiment. None of these fragmentations occurs within the presumed cyclic part of the peptide, a characteristic that corresponds to observations made when studying MS/MS fragmentation of protonated *S. aureus* AIPs. The b_4 ion at m/z 468.3 results from fragmentation of the peptide bond C-terminal to the threonine, which is the first residue outside the ring. The identity of the b_4 ion was verified by a MS^3 experiment that yielded b_2 ions (Fig. 4). The y_7 ion at m/z 738.5, observed in the MS/MS experiment, results from a preferred fragmentation of the peptide bond on the N-terminal side of proline that is also responsible for generating b_2 ions in the MS^3 experiment on b_4 ions. The y_7 ion comprises the cyclic portion of the peptide, making it 18 Da lighter than its theoretical linear counterpart. Subsequent fragmentation of the y_7 ion in an MS^3 experiment leads to y_5 and y_6 ions (m/zs 540.3 and 641.2) that also originate from bond dissociations outside the ring. These spectra provide strong evidence that the *S. intermedius* AIP is indeed a nonapeptide with a cyclized portion comprised of a lactone.

Sensitivity. Tests performed with synthetic factor α diluted into pure solutions of the MALDI matrix yielded informative MS/MS spectra (comparable to those shown in Fig. 2) at the 1 fmol level, i.e., at 1 nM concentration. The sensitivity was reduced ≈30-fold when the same peptide was introduced into suspensions of diploid yeast cells. Biologic activity assays for the AIPs suggest concentrations on the order of 30 nM in supernatants of late logarithmic cultures (10^9 cells per ml) (36, 39). AIP concentrations from a *S. epidermidis* strain were also reported to be in the same range (49).

Discussion

The present method is based on the ability of MALDI-ion trap MS to separate specified peptide ions from a complex and noisy mixture and to convert these selected peptide ions into a few informative fragment species with low noise background. Resonant excitation within the ion trap provides an efficient method to cleave peptide bonds at preferred positions, leading to relatively simple fragmentation signatures with high signal-to-noise ratios. Key to the success of the approach is the very small fraction of the total sample that is consumed to obtain each multistage mass spectrum. Consequently, we are able to test a large number of different hypotheses (>100) on a given sample before it is depleted. It is of interest to compare the present approach for testing hypotheses with alternatives that use LC-MS/MS (ref. 50 and references cited therein) where the number of hypotheses that can be tested is limited by the chromatographic peak width and the time required to acquire an MS/MS spectrum. For example, a combination of isotope-coded affinity tag (ICAT) methodology and online HPLC-MS/MS was recently used to test for the presence of a protein of interest from a complex mixture of proteins. In this case, it was possible to test for the presence of up to four peptides in a given LC run (compare with >100 tests by using the present method). The low utilization and stability of MALDI samples allow us to test hypotheses until we have exhausted many of the alternatives or even allow us to return to the problem after weeks of reflection. Any instrumentation with the properties outlined above should be capable of carrying out hypothesis-driven experiments of type described. Possibilities include Quadrupole quadrupole time-of-flight (Qq-TOF), TOF-TOF, and Fourier transform on cyclotron resonance (FT-ICR) analyzers.

The method proved extremely facile for yeast random spore analyses as well as for tetrad analyses that require testing for diploid contaminants. Technical problems that result from ambiguous halos around closely spaced colonies could be readily overcome by applying this on-the-spot mass spectrometric procedure. Although the present hypothesis driven multistage-MS approach for assaying mating pheromones from yeast colonies does not require any purification, concentration, or desalting steps, we found such steps to be useful for the analysis of Staphylococcal AIPs from liquid culture supernatants. A fast (≈1 min) and simple ZipTip procedure performed with small culture volumes (0.01–1 ml) proved adequate. Hypothetical masses that form the basis for any hypothesis-driven multistage-MS experiment have to be assessed carefully as the example of the natriated group-II-AIP ions demonstrates. The *S. intermedius* AIP is the only AIP in our study that contains a residue with a highly basic side chain (arginine). The presence of this arginine residue may explain why this AIP can readily be observed in single-stage MS mode with samples prepared from crude culture supernatants. Because the intensities of fragment ions of these modified, nontryptic peptide ions are difficult to predict, synthetic peptides, rather than database searches, were used to

increase the confidence level of our results. Although no synthetic form of the *S. intermedius* AIP was available for analysis, the MS^2 and MS^3 experiments of the natural AIP (Fig. 4) unambiguously characterize it as a nonapeptide lactone, which is the first such peptide characterized in *agr* signaling. This finding has important implications for understanding the detailed interaction of AIPs with their receptor. It has previously been demonstrated that the interaction of AIPs with the receptor, AgrC, is reversible and competitive (51), but it was not determined whether or not this interaction involved a transient covalent linkage step. In principle, such a step is conceivable because the *S. aureus* AIPs contain a reactive thioester linkage. The fact that we now have characterized a *S. intermedius* AIP lactone, which has much lower reactivity than a thioester, provides evidence against such a covalent interaction model. The use of lactone peptides for quorum sensing was also recently shown in the Gram-positive bacterium, *Enterococcus faecalis* (52).

Conclusion

Clearly, the method presented here is not limited to the detection of secreted peptides. It has the potential to be used for a very broad range of applications that include detection of any protein via its proteolytic fragments. Indeed, when the mass and fragmentation behavior of a specified peptide is known, hypothesis-driven multistage MS functions in a manner analogous to Western blotting, but with the potential for greater speed and throughput, while eliminating the need for a specific Ab.

We thank Tom Muir (The Rockefeller University) and Richard P. Novick (New York University) for generous support that included access to materials and fruitful discussions, and Fred Cross and Michael P. Rout (The Rockefeller University) for sage advice. This work was supported by National Institutes of Health Grants RR00862 and CA89810. G.J.L. was supported by the Medical Scientist Training Program (Grant GM07739). M.K. thanks the Max Planck Society (Germany) for support.

1. Fenselau, C. & Demirev, P. A. (2001) *Mass Spectrom. Rev.* **20,** 157–171.
2. Demirev, P. A., Ramirez, J. & Fenselau, C. (2001) *Anal. Chem.* **73,** 5725–5731.
3. Kratchmarova, I., Kalume, D. E., Blagoev, B., Scherer, P. E., Podtelejnikov, A. V., Molina, H., Bickel, P. E., Andersen, J. S., Fernandez, M. M., Bunkenborg, J., *et al.* (2002) *Mol. Cell Proteomics* **1,** 213–222.
4. Krutchinsky, A. N. & Chait, B. T. (2002) *J. Am. Soc. Mass Spectrom.* **13,** 129–134.
5. Barnett, D. A., Ding, L., Ells, B., Purves, R. W. & Guevremont, R. (2002) *Rapid Commun. Mass Spectrom.* **16,** 676–680.
6. Morris, H. R., Paxton, T., Panico, M., McDowell, R. & Dell, A. (1997) *J. Protein Chem.* **16,** 469–479.
7. McLafferty, F. W. (1983) *Tandem Mass Spectrometry* (Wiley, New York).
8. McLuckey, S., ed. (2001) *Int. J. Mass Spectrom.* **212,** 1–551.
9. Krutchinsky, A. N., Kalkum, M. & Chait, B. T. (2001) *Anal. Chem.* **73,** 5066–5077.
10. Gooday, G. W. (1974) *Annu. Rev. Biochem.* **43,** 35–87.
11. Wilkinson, L. E. & Pringle, J. R. (1974) *Exp. Cell Res.* **89,** 175–187.
12. Masui, Y., Chino, N., Sakakibara, S., Tanaka, T., Murakami, T. & Kita, H. (1977) *Biochem. Biophys. Res. Commun.* **78,** 534–538.
13. Hirsch, J. P. & Cross, F. R. (1992) *BioEssays* **14,** 367–373.
14. Kurjan, J. (1992) *Annu. Rev. Biochem.* **61,** 1097–1129.
15. Cross, F., Hartwell, L. H., Jackson, C. & Konopka, J. B. (1988) *Annu. Rev. Cell Biol.* **4,** 429–457.
16. Sprague, G. F., Jr. & Herskowitz, I. (1981) *J. Mol. Biol.* **153,** 305–321.
17. Huxley, C., Green, E. D. & Dunham, I. (1990) *Trends Genet.* **6,** 236.
18. Chan, R. K. & Otte, C. A. (1982) *Mol. Cell. Biol.* **2,** 21–29.
19. Chan, R. K. & Otte, C. A. (1982) *Mol. Cell. Biol.* **2,** 11–20.
20. Crane, J. K. (1999) *Clin. Lab. Med.* **19,** 583–599.
21. Sharma, S. & Verma, K. K. (2001) *Indian J. Pediatr.* **68,** Suppl. 3, S46–S50.
22. Giamarellou, H. (2002) *J. Hosp. Infect.* **50,** 91–105.
23. Llewelyn, M. & Cohen, J. (2002) *Lancet Infect. Dis.* **2,** 156–162.
24. Taskapan, M. O. & Kumar, P. (2000) *Ann. Allergy Asthma Immunol.* **84,** 3–10.
25. Miller, M. B. & Bassler, B. L. (2001) *Annu. Rev. Microbiol.* **55,** 165–199.
26. Winzer, K. & Williams, P. (2001) *Int. J. Med. Microbiol.* **291,** 131–143.
27. Winzer, K., Hardie, K. R. & Williams, P. (2002) *Curr. Opin. Microbiol.* **5,** 216–222.
28. Dunny, G. M. & Winans, S. C. (1999) *Cell-Cell Signaling in Bacteria* (Am. Soc. Microbiol., Washington, DC).
29. Novick, R. P., Projan, S. J., Kornblum, J., Ross, H. F., Ji, G., Kreiswirth, B., Vandenesch, F. & Moghazeh, S. (1995) *Mol. Gen. Genet.* **248,** 446–458.
30. Ji, G., Beavis, R. C. & Novick, R. P. (1995) *Proc. Natl. Acad. Sci. USA* **92,** 12055–12059.
31. Morfeldt, E., Janzon, L., Arvidson, S. & Lofdahl, S. (1988) *Mol. Gen. Genet.* **211,** 435–440.
32. Jarraud, S., Lyon, G. J., Figueiredo, A. M., Gerard, L., Vandenesch, F., Etienne, J., Muir, T. W. & Novick, R. P. (2000) *J. Bacteriol.* **182,** 6517–6522.
33. Dufour, P., Jarraud, S., Vandenesch, F., Greenland, T., Novick, R. P., Bes, M., Etienne, J. & Lina, G. (2002) *J. Bacteriol.* **184,** 1180–1186.
34. Ji, G., Beavis, R. & Novick, R. P. (1997) *Science* **276,** 2027–2030.
35. Brook, I. (1999) *Crit. Rev. Microbiol.* **25,** 155–172.
36. Lyon, G. J., Mayville, P., Muir, T. W. & Novick, R. P. (2000) *Proc. Natl. Acad. Sci. USA* **97,** 13330–13335.
37. Novick, R. P. (1991) *Methods Enzymol.* **204,** 587–636.
38. Mayville, P., Ji, G., Beavis, R., Yang, H., Goger, M., Novick, R. P. & Muir, T. W. (1999) *Proc. Natl. Acad. Sci. USA* **96,** 1218–1223.
39. Lyon, G. J., Wright, J. S., Muir, T. W. & Novick, R. P. (2002) *Biochemistry* **41,** 10095–10104.
40. Qin, J. & Chait, B. T. (1995) *J. Am. Chem. Soc.* **117,** 5411–5412.
41. Qin, J. & Chait, B. T. (1999) *Int. J. Mass Spectrom.* **191,** 313–320.
42. Goffeau, A., Barrell, B. G., Bussey, H., Davis, R. W., Dujon, B., Feldmann, H., Galibert, F., Hoheisel, J. D., Jacq, C., Johnston, M., *et al.* (1996) *Science* **274,** 546–567.
43. Philippsen, P., Kleine, K., Pohlmann, R., Dusterhoft, A., Hamberg, K., Hegemann, J. H., Obermaier, B., Urrestarazu, L. A., Aert, R., Albermann, K., *et al.* (1997) *Nature* **387,** 93–98.
44. Jacq, C., Alt-Morbe, J., Andre, B., Arnold, W., Bahr, A., Ballesta, J. P., Bargues, M., Baron, L., Becker, A., Biteau, N., *et al.* (1997) *Nature* **387,** 75–78.
45. Michaelis, S. & Herskowitz, I. (1988) *Mol. Cell. Biol.* **8,** 1309–1318.
46. Singh, A., Chen, E. Y., Lugovoy, J. M., Chang, C. N., Hitzeman, R. A. & Seeburg, P. H. (1983) *Nucleic Acids Res.* **11,** 4049–4063.
47. Kurjan, J. & Herskowitz, I. (1982) *Cell* **30,** 933–943.
48. Kurjan, J. (1985) *Mol. Cell. Biol.* **5,** 787–796.
49. Saenz, H. L., Augsburger, V., Vuong, C., Jack, R. W., Gotz, F. & Otto, M. (2000) *Arch. Microbiol.* **174,** 452–455.
50. Arnott, D., Kishiyama, A., Luis, E. A., Ludlum, S. G., Marsters, J. C., Jr., & Stults, J. T. (2002) *Mol. Cell Proteomics* **1,** 148–156.
51. Lyon, G. J., Wright, J. S., Christopoulos, A., Novick, R. P. & Muir, T. W. (2002) *J. Biol. Chem.* **277,** 6247–6253.
52. Nakayama, J., Cao, Y., Horii, T., Sakuda, S., Akkermans, A. D., de Vos, W. M. & Nagasawa, H. (2001) *Mol. Microbiol.* **41,** 145–154.
53. Biemann, K. (1990) *Methods Enzymol.* **193,** 886–887.